Article

Novel methodology & optimization of heat pump efficiency through stochastic finite element analysis and circular statistics

Debashis Chatterjee[*], **Subhrajit Saha**

Department of Statistics, Visva Bharati University, Santiniketan 731235, India
* Corresponding author: Debashis Chatterjee, debashis.chatterjee@visva-bharati.ac.in

Abstract: This research introduces a novel framework integrating stochastic finite element analysis (FEA) with advanced circular statistical methods to optimize heat pump efficiency under material uncertainties. The proposed methodologies and optimization focus on balancing the mean efficiency and variability by adjusting the concentration parameter of the Von Mises distribution, which models directional variability in thermal conductivity. The study highlights the superiority of the Von Mises distribution in achieving more consistent and efficient thermal performance compared to the uniform distribution. We also conducted a sensitivity analysis of the parameters for further insights. The results show that optimal tuning of the concentration parameter can significantly reduce efficiency variability while maintaining a mean efficiency above the desired threshold. This demonstrates the importance of considering both stochastic effects and directional consistency in thermal systems, providing robust and reliable design strategies.

Keywords: stochastic finite element analysis (FEA); circular statistical methods; Von Mises distribution; thermal conductivity; heat pump efficiency

1. Introduction

The efficiency of thermal systems, particularly heat pumps, is pivotal in environmental sustainability and operational cost-effectiveness. Heat pumps are extensively used for heating and cooling in residential and industrial applications, where their efficiency directly impacts energy consumption and carbon emissions. As global energy efficiency standards tighten, optimizing the performance of heat pumps has become increasingly important. However, accurately predicting and optimizing heat pump performance remains challenging due to the variability in material properties such as thermal conductivity. These material properties are not only stochastic but also exhibit directional variability, introducing complexities that are often overlooked in traditional modeling approaches.

Researchers have made significant strides in optimizing heat pump systems through various design and operational strategies in recent years. For example, Huang et al. [1] optimized integrating photovoltaic systems, heat pumps, thermal storage, and electric vehicles in residential building clusters to create self-sufficient energy ecosystems in Sweden. Similarly, Ahmed et al. [2] employed data-driven machine learning techniques to optimize the design and operational controls of borehole heat exchanger-coupled heat pumps, highlighting the potential of combining optimization algorithms with sustainable technology.

However, while advancing the field, these studies often fail to account for the directional variability of material properties such as thermal conductivity. Most heat

pump optimization approaches, including those by Halilovic et al. [3] and Li et al. [4], have focused on optimizing spatial layouts, well configurations, or heat sink designs. Tancabel et al. [5], for instance, conducted a multi-physics analysis to optimize heat exchangers with novel non-round tubes, while Zhang et al. [6] improved the grid connection performance of pump turbines by optimizing the guide vane profile. Though these methods enhance system-level performance, they typically rely on linear or isotropic assumptions about material properties, which limit their applicability in anisotropic materials.

This research builds on these foundational studies by addressing a gap in the literature: the role of directional variability in thermal conductivity. By integrating stochastic finite element analysis (FEA) with circular statistical methods, we provide a novel framework for evaluating and optimizing heat pump efficiency under material uncertainty. Unlike prior works focusing on system optimization from a macroscopic or operational perspective, this study delves into the material-level properties governing heat transfer. With its ability to model concentrated angular data, the Von Mises distribution offers a more realistic representation of directional consistency in thermal properties, particularly in anisotropic materials.

A major gap in the existing literature is the lack of adequate modeling approaches that account for the directional properties of thermal conductivity. Current modeling techniques often rely on linear statistical methods or assume isotropic conditions, which neglect the complexity introduced by anisotropic materials. Moreover, these traditional models fail to capture the stochastic nature of material properties, which are subject to uncertainty due to manufacturing processes, environmental conditions, and aging. When combined with stochastic variability, the directional aspects of thermal conductivity can significantly affect heat pump efficiency, yet these factors are often overlooked in performance predictions. Recent advancements in circular statistics (see, e.g., Mardia and Jupp [7] and Jammalamadaka and SenGupta [8]) provide a promising framework for addressing this gap. Circular statistics allow for modeling angular variables such as phase angles and material orientations, making them ideal for analyzing directional properties in anisotropic materials. Specifically, the Von Mises distribution—a circular analog of the normal distribution—offers a robust method for capturing the concentration of directional data around a mean direction. By incorporating circular statistics, we can move beyond traditional scalar-based models and develop a more accurate representation of thermal conductivity in anisotropic systems. In addition to addressing the modeling gap, our research complements previous optimization studies, such as those by Pejman et al. [9] and Chaoran et al. [10], which explored hybrid topology/shape optimization for microvascular composites and machine learning-driven ground source heat pump optimizations, respectively. While these studies advanced heat pump performance through design and operational improvements, they did not fully account for material properties' anisotropic and stochastic nature. Our research takes another very different route, incorporating circular statistics. Our research introduces a new dimension to this work by incorporating stochastic effects and directional consistency, offering a more robust and reliable approach to optimizing heat pump systems.

In this study, we conduct a comprehensive simulation analysis that compares the performance of heat pumps when thermal conductivity is modeled using both the

uniform and Von Mises distributions. The latter, characterized by its concentration parameter κ, is hypothesized to provide superior thermal performance by reducing variability and optimizing directional heat flow. Through extensive simulations, we demonstrate that the Von Mises distribution outperforms the uniform distribution in minimizing thermal losses and enhancing the reliability of heat pump performance. These findings are in line with other studies, such as those by Kudela et al. [11] and Ranganayakulu and Seetharamu [12], which emphasized the importance of accounting for geographic, climatic, and material conditions in thermal system performance.

Our research significantly contributes to heat pump optimization by introducing an innovative modeling framework incorporating stochastic and directional variability. The results highlight the importance of considering these factors in future designs and suggest that circular statistical methods, particularly the Von Mises distribution, should be prioritized when analyzing and optimizing thermal systems.

2. Related works

The optimization of heat pump systems has been a focus of significant research in recent years, with various studies addressing different aspects of their performance and design. Aakbarzadeh et al. [13] introduced bi-functional heat pumps (bi-FHPs) as an energy-efficient solution for heating and cooling across multiple sectors. Their work highlights the potential of bi-FHPs to reduce costs and improve sustainability, although environmental and operational factors can significantly influence performance outcomes. Xu et al. [14] developed a semi-theoretical model for fixed-speed air source heat pumps (ASHPs), considering no-load power consumption, cycling losses, and defrost effects. Their model enables dynamic simulations and energy efficiency analyses with less than 10% error in predicting seasonal performance, thus offering valuable tools for better understanding the energy dynamics of ASHPs. Chua et al. [15] provided a comprehensive review of advancements in heat pump systems, emphasizing innovations in cycle design, working fluids, and hybrid systems. Their work underscored the importance of developments such as heat-driven ejectors and improved compressor technologies, both of which have significantly enhanced the performance of modern heat pumps. Ruhnau et al. [16] used the "When2Heat" dataset to generate synthetic national time series for heat demand and the coefficient of performance (COP) of electric heat pumps in 16 European countries from 2008 to 2018. Their work is invaluable for analyzing temporal variability in heat pump power consumption across diverse energy systems.

The performance of ground source heat pump (GSHP) systems has also been extensively studied. Noorollahi [17] reviewed key parameters affecting the performance of ground heat exchangers (GHE), such as inlet temperature, fluid velocity, and pipe arrangement. Their findings showed that properly optimizing these factors is crucial to enhancing system efficiency. Casasso et al. [18] focused on the rising importance of geothermal heat pumps in light of increasing fossil fuel costs and the need for CO_2 emissions reduction. They highlighted how factors like borehole heat exchanger (BHE) length, heat carrier fluid, and soil properties critically influence system reliability and performance.

Air source heat pumps (ASHPs) have also been extensively examined. Chesser et al. [19] assessed the performance of ASHPs in retrofitted Irish homes, noting a discrepancy between actual COP values and manufacturer estimates. They employed statistical models to analyze the factors contributing to this underperformance, offering insights into how these systems can be better optimized for specific applications. Singh et al. [20] addressed the barriers to heat pump adoption in the UK, where conventional boilers still dominate despite the superior energy efficiency of heat pumps. Their study explored various factors influencing consumer choice, including operational costs, reliability, and environmental concerns. Dongellini et al. [21] presented a numerical model for evaluating the seasonal performance of electric air to water heat pumps, compliant with European standards. Their research emphasized the importance of operational modes and appropriate sizing, particularly for inverter-driven and multi-compressor systems, to maximize seasonal efficiency.

Borehole spacing in GSHP systems has also garnered attention. Cai et al. [22] re-evaluated the optimal borehole spacing for long-term performance, recommending a 6-meter spacing to prevent heat accumulation and ensure better system efficiency over 20 years. This study underscored the significance of considering long-term thermal effects in system design. Reiners et al. [23] studied heat pumps in ultralow temperature district heating (ULTDH) networks, demonstrating that these systems can operate up to twice as efficiently at lower temperature spreads compared to geothermal probes, highlighting the benefits of reduced temperature differentials in district heating applications.

The efficiency of heat pump water heaters (HPWHs) has been explored by Willem et al. [24], who reviewed technological advancements that could potentially increase COP values from the current 1.8–2.5 range to 2.8–5.5. Their review addressed the technical challenges that must be overcome to improve the energy efficiency of HPWH systems. Hu et al. [25] compared three centrifugal heat pump systems with waste heat recovery, finding that a two-cycle parallel system achieved up to 19% improvement in COP, making it particularly suitable for industrial applications where heat recovery is crucial. Cold climate applications of heat pumps were examined by Gibb et al. [26], who demonstrated that air-source heat pumps (ASHPs) remain more efficient than fossil fuel heating systems, even in sub-zero temperatures. Their work highlights the significant benefits of ASHPs in typical European winter conditions, although further analysis is needed for extreme climates. Sarbu et al. [27] reviewed the energy-saving potential of ground-source heat pumps (GSHPs) across different climates, including detailed analyses of surface water heat pumps (SWHP), groundwater heat pumps (GWHP), and ground-coupled heat pumps (GCHP). Their study underscored the adaptability of GSHPs to both cold and hot climates, offering significant environmental and economic benefits. Santa et al. [28] developed a validated mathematical model for water-to-water heat pump systems, achieving an average error of just 1.73% when compared to experimental data. Their model is useful for determining the optimal operating point to maximize system efficiency. Gao et al. [29] analyzed 26 GSHP systems in southwest and western China, finding suboptimal performance with COP values below 3.0. They recommended the adoption of ground-coupled heat pump (GCHP) systems for improved energy efficiency in these regions. Saeidi et al. [30] improved geothermal heat pump efficiency by incorporating high

thermal conductivity materials into GHEs, achieving a 37% increase in overall efficiency. Their study emphasized the role of optimized soil moisture content and enhanced material conductivity in boosting system performance. The effect of frost prevention on heat-source-tower heat pump systems was examined by Cheng et al. [31], who demonstrated that system efficiency increased by 5% to 11% under antifreeze conditions, providing valuable design insights for cold-weather applications. Corbean et al. [32] introduced an innovative dual-source heat pump (DSHP) that switches between air and ground sources, achieving comparable efficiency to GSHPs at a fraction of the installation cost, making it a promising solution for multi-purpose heating and cooling systems. Wood et al. [33] explored using energy piles as sustainable heating solutions for residential buildings. Their findings indicated that concrete piles could economically provide the required heat while maintaining ground temperature stability. Eswiasi et al. [34] reviewed the thermal efficiency of vertical ground heat exchangers in GSHP systems, concluding that increasing borehole and pipe diameters, along with optimized configurations, significantly enhances thermal performance. De Le´on-Ruiz and Carvajal-Mariscal [35] introduced a novel thermal capacity metric to assess heat pump performance, combining it with COP to set minimum operational standards for energy demand fulfillment, further advancing the understanding of heat pump system performance.

These diverse studies collectively contribute to the ongoing development of heat pump technologies, offering a range of methodologies and insights that address both system design and operational strategies. This body of work forms the foundation upon which this research builds, integrating stochastic finite element analysis and circular statistical methods to provide a more comprehensive framework for heat pump optimization.

3. Objective and novelty of the research

The primary objective of this research is to develop a comprehensive analytical framework that integrates stochastic finite element analysis (FEA) with advanced circular statistical methods, specifically emphasizing the superiority of the Von Mises distribution to optimize the performance of heat pumps under material uncertainty. This approach is particularly novel for several reasons:

Incorporation of Directional Variability with Von Mises Distribution: Unlike traditional methods that treat thermal conductivity as a scalar quantity, this research models it as a stochastic process with a directional component using the Von Mises distribution. The concentration of directional data around a mean direction provided by the Von Mises distribution offers a more accurate representation of anisotropic materials and their impact on thermal performance than the uniform distribution.

Application of Circular Statistics for Enhanced Accuracy: Circular statistical methods, particularly the Von Mises distribution, are introduced to analyze the angular components of thermal conductivity. This approach significantly differs from linear statistical methods, providing a more precise analysis of phenomena such as phase shifts and material orientations, thereby improving thermal system design.

Integration of Circular Statistics with Stochastic FEA: The research directly integrates advanced circular statistical techniques into the stochastic FEA process. By

leveraging the Von Mises distribution, this integration allows for a detailed exploration of how directional consistency and randomness in material properties affect the heat pump's overall efficiency, a novel contribution to thermal system modeling.

Optimization to improve the heat pump's performance: The optimization pertains to improving the heat pump's performance by balancing efficiency and variability under material uncertainties. The optimization is achieved by tuning the concentration parameter κ of the Von Mises distribution, which models directional variability in thermal conductivity. Specifically, the optimization objective is to minimize the standard deviation (variability) of the efficiency while ensuring that the mean efficiency remains above a certain threshold, $\eta_{\text{threshold}} = 1.0$. The optimization method involves a stochastic finite element analysis (FEA) combined with circular statistical analysis to identify the optimal κ. Performance improvements after optimization are quantitatively demonstrated by comparing the variability before and after optimization. For example, by adjusting κ, the variability in efficiency was reduced by approximately 80.13%, providing more consistent heat pump operation with minimal efficiency loss.

Performance Evaluation & Sensitivity Analysis: The study provides a more robust and realistic evaluation of heat pump performance by treating material properties as random variables and employing the Von Mises distribution for circular statistical analysis. This is crucial for developing reliable and efficient thermal systems in practical applications, particularly in environments where material properties are uncertain. The sensitivity analysis indicates that while mean efficiency $\eta(\kappa)$ remains stable, variability in efficiency rises with increasing κ, suggesting that higher κ values, correlating with greater directional concentration, lead to increased performance variability. The sensitivity coefficient $S\kappa$ identifies critical regions where small changes in κ significantly impact efficiency.

The novel combination of stochastic FEA and the superior circular statistical tools, particularly the 3 Von Mises distribution, represents a significant advancement in the field of thermal system design. It offers new insights and methodologies for optimizing performance under conditions of uncertainty, setting a new standard for the analysis and design of efficient thermal systems.

4. Theoretical framework

4.1. Thermodynamic principals

The heat pump cycle is modeled using fundamental thermodynamic equations. The Carnot cycle serves as a basis, with modifications for real-world inefficiencies. The energy balance equation for a differential volume element in the heat pump is expressed as:

$$\frac{dQ}{dt} = m \cdot c_p \cdot \frac{dT}{dt} + \sigma dW(t)$$

where:

Q is the heattransferrate,
m is the mass flowrate,

c_p is the specificheatcapacity,

T is the temperature,

σ is the volatility term,

W(t) is a Wiener process representing the rmalfluctuations.

4.2. Stochastic modelling

Key material properties, such as thermal conductivity$k$, are modeled as random fields:

$$k_i \sim N(\overline{k}, \sigma_k^2)$$

where:

$\overline{k}$ is mean the mean thermal conductivity,

σ_k^2 is the variance.

For each element i in the mesh, the thermal conductivity k_i is independently sampled from this distribution.

The governing equation of heat conduction in a one-dimensional rod without internal heat generation is:

$$\frac{-d}{dx}\left(k(x)\frac{dT(x)}{dx}\right) = 0$$

Given that, $k(x)$ is now a stochastic process, this equation becomes:

$$\frac{-d}{dx}\left(k_i\frac{dT_i(x)}{dx}\right) = 0$$

where k_i represents the random thermal conductivity in element i and $T_i(x)$ is the temperature distribution in that element.

5. Methodology: Part 1

5.1. Design and geometry of the heat pump

The novel heat pump design features a unique geometrical configuration optimized for efficient heat transfer. The geometry is modeled in cylindrical and spherical coordinates to account for varying heat flow patterns. The design is implemented in a Python based simulation environment using libraries such as *NumPy* and *SciPy* for FEA.

5.2. Stochastic finite element analysis (FEA)

The rod is discretized into (N) elements in the finite element method, and piecewise linear basis functions approximate the temperature distribution. The weak form of the governing equation for each element leads to the system of equations:

$$K_i T = F_i$$

where:

K_i is the local stiffness matrix for element i, which depends on the random thermal conductivity K_i,

T is the vector of nodal temperatures,

F_i is the force vector, representing boundary conditions.

Multiple simulations (Monte Carlo method) are performed to account for the randomness in thermal conductivity. For each simulation j:

Sample K_i: A Set of $k_i^{(j)}$ values is drawn from $(N(\overline{k}, \sigma_k^2)$

The system of linear equations is solved to find the temperature distribution $T_i^{(j)}(x)$ corresponding to the sampled $k_i^{(j)}$.

After running M simulations, the temperature distribution at each node is analyzed to compute the mean and variance:

$$\mu_T(x) = \frac{1}{M} \sum_{j=1}^{M} T^{(j)}(x)$$

$$\sigma_T^2(x) = \frac{1}{M} \sum_{j=1}^{M} \left(T^{(j)}(x) - \mu_T(x) \right)^2$$

$$\sigma_T(x) = \sqrt{\sigma_T^2(x)}$$

6. Methodology: Part 2: Incorporating circular statistical tools

6.1. Introduction to circular statistics in thermal systems

In classical statistics, data points typically lie linearly (e.g., temperatures, lengths). However, properties in thermal systems, such as phase angles in wave propagation or orientations in anisotropic materials, are better represented on a circular scale. Circular statistics provide the tools necessary to analyze such data, where the primary feature is the periodic nature of the domain (e.g., angles ranging from 0 to 2π.

In the context of this study, we introduce circular statistical methods to analyze potential angular components of thermal fluctuations, orientations in material anisotropy, or phase shifts in thermal waves.

6.2. Motivation for using the Von Mises distribution

While the uniform distribution is useful for modeling angular data where all directions are equally likely, it may not fully capture scenarios where there is a preferred direction or orientation. The Von Mises distribution, often referred to as the circular normal distribution, is the maximum entropy distribution for circular data under a given mean direction and concentration parameter constraint. This makes it particularly useful when modeling directional data with some degree of clustering around a mean direction.

The Von Mises distribution is defined as:

$$f(\theta; \mu, \kappa) = \frac{e^{\kappa cos(\theta - \mu)}}{2\pi I_0(\kappa)}$$

where:

θ is the angular variable,

μ is the mean direction,

κ is the concentration parameter (analogous to the inverse of the variance in the normal distribution,

$I_0(\kappa)$ is the modified Bessel function of the first kind of order 0.

The Von Mises distribution is used in this study to model scenarios where the thermal conductivity $k(x)$ not only varies stochastically but also exhibits a directional preference. This allows us to explore how anisotropic properties with specific directional tendencies affect thermal performance.

6.3. Modeling thermal fluctuations as circular data using uniform and Von Mises distributions

Consider a scenario where the thermal conductivity $k(x)$ not only varies stochastically but also has a directional component, possibly representing anisotropy in the material or the orientation of thermal flow. This directional component can be modeled using an angular variable $\theta(x)$, where $\theta(x)$ represents the direction or phase angle of the thermal conductivity at position x.

We now model $\theta(x)$ as a random variable on the circle using both the uniform distribution and the Von Mises distribution:

Uniform Distribution

$$\theta(x) \sim \text{Uniform}(0, 2\pi)$$

This assumes that the thermal conductivity direction is equally likely in any direction.

Von Mises Distribution

$$\theta(x) \sim \text{Von Mises}(\mu, \kappa)$$

Here, μ represents the preferred direction of thermal conductivity, and κ indicates how strongly the directions are concentrated around, μ. A higher κ value suggests that the thermal conductivity is more likely to be aligned close to μ, whereas a lower κ value indicates more spread around the circle.

The thermal conductivity can now be expressed as a function of both magnitude and direction for both distributions:

$$k(x) = k_0(x) \cdot \cos\big(\theta(x)\big)$$

where $k_0(x)$ is the magnitude of the thermal conductivity, potentially modeled as a random variable as in Part 1.

6.4. Circular statistical analysis of thermal conductivity

To analyze the angular data $\theta(x)$, we apply circular statistical methods, including calculating the circular mean and the resultant vector length, which provides insight into the concentration of the directional data.

The circular mean $\overline{\theta}$ of the angles $\theta(x)$ at different positions x is given by:

$$\overline{\theta} = arg\left(\sum_x \cos\big(\theta(x)\big) + i \sum_x \sin\big(\theta(x)\big) \right)$$

The resultant vector length R, which indicates the degree of concentration of the angles around the mean direction is defined as:

$$R = \frac{1}{N} \sqrt{\left(\sum_x cos(\theta(x)) \right)^2 + \left(\sum_x sin(\theta(x)) \right)^2}$$

where, N is the number of positions x considered.

By comparing the results from both the uniform and Von Mises distributions, we can assess how different models of directional data influence the thermal conductivity's directional consistency and its impact on thermal performance.

6.5. Incorporating circular statistics in FEA

In the context of Finite Element Analysis, we modify the thermal conductivity term to include the directional component modeled by both distributions:

$$\frac{-d}{dx} \left(k_0(x) cos(\theta(x)) \frac{dT(x)}{dx} \right) = 0$$

This modification reflects the anisotropic or directional influence on heat conduction, where $\theta(x)$ represents the orientation of the material's thermal properties.

The boundary conditions remain as:

$$T(0) = T_{\text{cold}} = 0°C, T(L) = T_{\text{hot}} = 100°C$$

The simulation is repeated 100 times with $\theta(x)$ sampled uniformly and from the Von Mises distribution. The circular statistics of $\theta(x)$ are then computed to assess the impact of directional properties on the temperature distribution.

6.6. Results: circular statistical analysis of thermal conductivity

The circular mean $\overline{\theta}$ and resultant vector length R are calculated for each simulation under both distributions, providing insight into the directional consistency of thermal conductivity across the rod.

6.7. Circular analysis of heat pump efficiency

To incorporate circular statistics in the analysis of heat pump efficiency, we examine how the angular variability $\theta(x)$ influences the overall performance. Specifically, we analyze the relationship between the circular mean $\overline{\theta}$ and the efficiency η:

Circular-Efficiency Relationship: Investigate if the efficiency η shows any dependence on the circular mean $\overline{\theta}$ of the angles $\theta(x)$.

Circular Variability Impact: Assess the impact of the resultant vector length R on the stability of efficiency. A lower R might indicate higher variability in efficiency due to more dispersed directional influences.

Comparison Between Distributions: By comparing the results obtained from the uniform distribution and the Von Mises distribution, we can determine the sensitivity of heat pump efficiency to different models of directional data. With its ability to

model concentrated directions, the Von Mises distribution may provide deeper insights into the efficiency's dependency on directional anisotropy.

The circular statistical metrics and efficiency data are used to evaluate how directional properties influence the system's thermal performance under both the uniform and Von Mises distribution scenarios.

7. Stochastic finite element model with circular random variables

As shown in **Figure 1**, the rod is modeled as a vertical system consisting of N finite elements, where each element e_i has an associated thermal conductivity k_{e_i} and a heat flux q_{e_i}. The nodal temperatures at the top and bottom of the rod are fixed, with the temperature at the bottom $T(x_0)$ set to the cold sink temperature T_{cold} and the temperature at the top $T(x_N)$ set to the hot source temperature Thot.
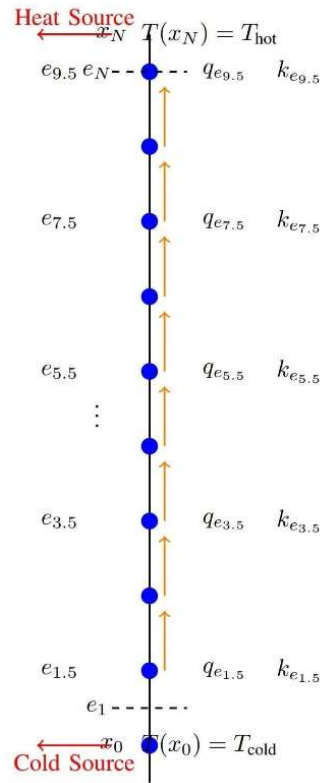

Figure 1. Vertical finite element model for heat conduction.

The rod is divided into N elements $e\ i$, with heat flowing from the hot source at $T \times N = T\ Hot$ to the cold sink at $T \times 0 = T\ Cold$. The heat flux $q\ e\ i$ for each element is indicated, and the thermal conductivity of each element k, e, i, is shown.

The heat flux, represented by the orange arrows between each element, shows the direction of heat transfer from the hot end to the cold end. The boundary conditions include a cold source at T_{Cold} (bottom) and a heat source at T_{Hot} (top), which are indicated by the red arrows.

The governing heat conduction equation is:

$$\frac{-d}{dx}\left(k(x)\frac{dT(x)}{dx}\right) = 0$$

where k(x) is the material's thermal conductivity in each element. In the finite element method, the weak form of this equation is solved to find the temperature distribution across the rod.

Each element is represented by a local stiffness matrix that depends on the thermal conductivity k_{e_i}, and the global system of equations for the entire rod is solved to find the nodal temperatures $T(x_i)$. The variation in kei across elements introduces stochastic effects in the heat transfer, which are analyzed in this study.

The diagram provides a clear visual representation of the heat flow between elements, the temperatures at the boundaries, and the role of thermal conductivity in determining the heat transfer efficiency across the rod.

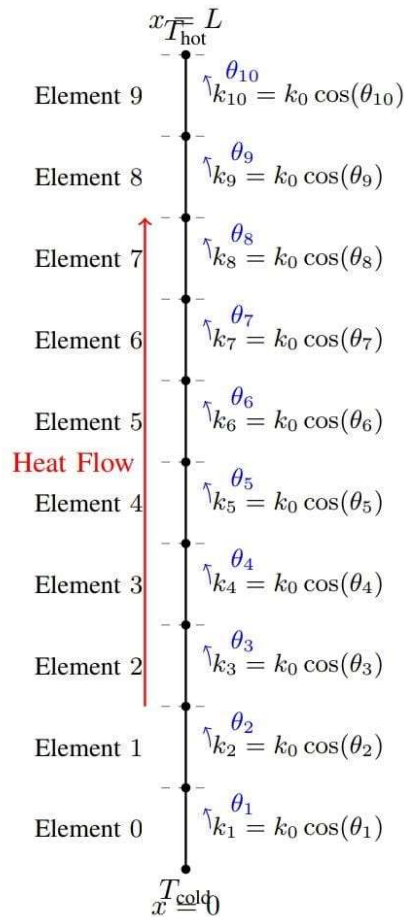**Finite element model incorporating circular statistical features**

Figure 2. Finite element model of the heat pump system showing mesh discretization into elements, boundary conditions (T_{Cold} and T_{Hot}), directional thermal conductivity with angles θ_i, and heat flow direction. The random angles θ_i incorporate the circular statistical features into the model.

The finite element model (FEM) of the heat pump system is illustrated in **Figure 2**. The model represents a one-dimensional rod of length L, discretized into N finite

elements of equal length $\Delta x = L/N$. Each node represents a point where the temperature is calculated.

- Geometry and Mesh Discretization: The rod is divided into N elements, with nodes at positions $x_0 = 0, x_1 = \Delta x, x_2 = 2\Delta x, \ldots, x_N = L$.

- Boundary Conditions:

$$T(x = 0) = T_{Cold},$$

$$T(x = L) = T_{Hot}$$

- Heat Flow Direction: In the context of heat pump operation, heat is transferred from the cold end ($x = 0$) to the hot end ($x = L$), against the natural temperature gradient, as indicated by the red arrow in the figure. This process requires external work input, consistent with the principles of heat pumps.

- Material Properties Assignment: Each element i is assigned a thermal conductivity k_i, which incorporates both stochastic and directional variability.

1) Incorporation of Circular Statistical Features:

To model the anisotropic and uncertain nature of the thermal conductivity, we introduce a directional component using circular statistics:

$$k_i = k_0 cos(\theta_i), i = 1,2, \ldots, N \tag{1}$$

where:

- k_0 is the magnitude of the thermal conductivity,

- θ_i is a random angle associated with element i, representing the directional variability,

- θ_i is modeled as a random variable following either a Uniform distribution $\theta_i \sim \text{Uniform}(0, 2\pi)$ or a Von Mises distribution $\theta_i \sim \text{VonMises}(\mu, \kappa)$.

The use of $cos(\theta_i)$ in Equation (1) introduces the directional dependence of thermal conductivity, effectively modeling anisotropic behavior. The random angles θ_i capture the variability in the material's directional properties, incorporating the circular statistical features into the FEM.

2) Finite Element Formulation

The governing equation for steady-state heat conduction in one dimension, considering the heat pump operation (where external work is applied to transfer heat from cold to hot), can be modified to include a source term representing the work input $Q_{\text{work}}(x)$:

$$\frac{-d}{dx}\left(k(x)\frac{dT(x)}{dx}\right) + Q_{\text{work}}(x) = 0 \tag{2}$$

In this simplified model, we may assume that the work input is uniformly distributed along the rod or consider it as part of the boundary conditions. For the purposes of our FEM, we focus on the effective thermal conductivity and its impact on the temperature distribution, acknowledging that the heat pump operation involves external work to maintain the temperature gradient against the natural flow of heat.

Discretizing the domain using the finite element method, we approximate the temperature distribution $T(x)$ using linear shape functions within each element. Applying the Galerkin method leads to a system of equations for the nodes:

$$KT = F \tag{3}$$

where:

- K is the global stiffness matrix, assembled from the elemental stiffness matrices k_i,
- T is the vector of nodal temperatures,
- F is the global force vector, incorporating boundary conditions and any source terms.

The elemental stiffness matrix for element i is given by:

$$K_i = \frac{k_i}{\Delta x}\begin{bmatrix} 1 & -1 \\ -1 & 1 \end{bmatrix} \tag{4}$$

3) Incorporation of Stochasticity and Directionality:

By substituting k_i from Equation (1) into the FEM formulation, we directly incorporate both stochasticity and directional variability into the model:

$$k_i = k_0 cos(\theta_i), \theta_i \begin{cases} Uniform(0,2\pi), \\ VonMises(\mu, \kappa) \end{cases} \tag{5}$$

This approach allows us to model the uncertainty in material properties due to manufacturing variations or inherent material anisotropy. The circular statistical distributions used for θ_i capture the likelihood of certain directional orientations within the material.

4) Simulation Procedure:

The simulation involves the following steps:

i. Initialization: Define the number of elements N, the length L, and the thermal conductivity magnitude k_0.

ii. Sampling of Angles: For each element i, sample θ_i from the chosen circular distribution.

iii. Assembly of Stiffness Matrix: Compute k_i using Equation (1) and assemble the global stiffness matrix K.

iv. Application of Boundary Conditions: Incorporate the boundary conditions into the system.

v. Solution: Solve the linear system in Equation (3) to find the temperature distribution T.

vi. Repetition: Repeat the simulation multiple times to perform a stochastic analysis, capturing the variability due to the random angles θ_i.

5) Role of Circular Statistics: The use of circular statistical tools is crucial for accurately modeling the directional variability of thermal conductivity:

- The Uniform distribution assumes that all directions are equally likely, representing a material with isotropic random orientation.
- The Von Mises distribution allows for modeling materials with a preferred orientation, with μ indicating the mean direction and κ controlling the concentration around μ.

By comparing the results obtained using these two distributions, we assess the impact of directional consistency and variability on the heat pump's efficiency.

6) Implications for Heat Pump Efficiency: The finite element model incorporating stochastic and directional variability provides insights into how material uncertainties affect thermal performance. The model helps in optimizing the heat pump design by:

- Identifying the importance of material anisotropy and preferred orientations.
- Quantifying the impact of directional variability on temperature distribution and heat flow.
- Guiding the selection of materials and manufacturing processes to achieve desired thermal properties.

The detailed finite element model and the incorporation of circular statistical features enhance the robustness of the simulation study, providing a comprehensive understanding of the factors influencing heat pump efficiency.

8. Optimization methodology

8.1. Optimization objectives

The initial objective was to optimize the heat pump efficiency η by varying the concentration parameter κ of the Von Mises distribution, with the expectation that higher κ (i.e., greater directional concentration) would lead to increased efficiency. However, the simulation results indicate that the maximum mean efficiency occurs at the lowest κ value (κ = 0.5). Given this, we re-evaluate our optimization objective to focus on:

1) Minimizing the Variability of Efficiency: Finding the κ that minimizes the standard deviation of efficiency σ_η, thereby achieving more consistent performance.

2) Balancing Efficiency and Consistency: Identifying a κ value that provides acceptable mean efficiency while minimizing variability.

Mathematically, the optimization problem is reformulated as:

$$\min_{\kappa} \sigma_\eta(\kappa) \tag{6}$$

subject to:

- ($\eta(\kappa) \geq \eta_{\text{threshold}}$), ensuring efficiency remains above a certain acceptable level.
- κ ≥ 0.

8.2. Optimization methods

To solve the revised optimization problem, we:

1) Parameter Sampling: Vary κ over the range [0.5, 10.0].

2) Stochastic Simulation: For each κ, perform stochastic simulations to compute η(κ) and $\sigma_\eta(\kappa)$.

3) Optimization: Identify the κ that minimizes $\sigma_\eta(\kappa)$ while maintaining η(κ) ≥ $\eta_{threshold}$.

8.3. Implementation details

We set $\eta_{threshold}$ = 1.0, representing the baseline acceptable efficiency level. The optimization seeks to find the smallest ση (κ) among κ values satisfying η(κ) ≥ 1.0.

8.4. Mathematical formulation

For each κ, we compute:

$$\eta(\kappa) = \frac{1}{M} \sum_{j=1}^{M} \eta^{(j)}(\kappa) \tag{7}$$

$$\sigma_\eta(\kappa) = \sqrt{\frac{1}{M-1} \sum_{j=1}^{M} \left(\eta^{(j)}(\kappa) - \eta(\kappa)\right)^2} \tag{8}$$

8.5. Performance improvement quantification

We quantify performance improvement in terms of reduced variability (Variability Reduction (VR) %):

$$VR = \left(\frac{\sigma_\eta(\kappa_{\text{baseline}}) - \sigma_\eta(\kappa_{\text{opt}})}{\sigma_\eta(\kappa_{\text{baseline}})}\right) \times 100\% \tag{9}$$

9. Simulation of the methodology incorporating circular statistics

The simulation process that implements the above methodology is outlined as follows:
A. Step 1: Initialization of Parameters
    Begin by defining the basic parameters of the simulation:
    - Length of the rod L and discretization into elements.
    - Mean thermal conductivity ($\bar{k}$) and its standard deviation (σ_k).
    - Two distributions for the angular variable $\theta(x)$: a uniform distribution across 0 to 2π and a Von Mises distribution with parameters μ and k.
B. Step 2: Circular Statistical Generation
    For each element in the rod:
    Generate $\theta(x)$ from both the uniform distribution Uniform$(0, 2\pi)$ and the Von Mises distribution (Von Mises(μ, κ).
    Calculate the thermal conductivity for each element using $k(x) = k_0(x)\cos(\theta(x))$ under both distributions.
A. Step 3: Finite Element Analysis with Circular Modification
    Modify the FEA process to incorporate the directional component:
    Use the modified thermal conductivity $k(x)$ in the FEA formulation for both the uniform and Von Mises distributions.
    Solve the temperature distribution $T(x)$ using the modified equation:

$$\frac{-\mathrm{d}}{\mathrm{dx}}\left(\mathrm{k_0(x)\cos\theta(x)}\frac{\mathrm{dT(x)}}{\mathrm{dx}}\right) = 0$$

Apply boundary conditions $\mathrm{T(0) = 0°C, T(L) = 100°C}$.

C. Step 4: Circular Statistical Analysis

After obtaining the temperature distribution:

- Calculate the circular mean $\overline{\theta}$ and resultant vector length R for the set of $\theta(x)$ values under both the uniform and Von Mises distributions.
- Assess the relationship between these circular statistics and the temperature distribution for each distribution.

B. Step 5: Heat Pump Efficiency Analysis

Finally, evaluate the heat pump efficiency η for each simulation:

- Compute the heat input Q_{in} and output Q_{out}.
- Calculate the efficiency η and analyze its correlation with the circular statistics $\overline{\theta}$ and R under both distributions.

D. Step 6: Repeating the Simulation

Repeat the entire simulation process 100 times for both distributions:

- Aggregate the results of $\eta, \overline{\theta}$ and R across simulations for both the uniform and Von Mises distributions.
- Perform statistical analysis on the aggregated results to conclude the directional effects on thermal conductivity and efficiency under each distribution.

This simulation framework provides a comprehensive approach to incorporating circular statistics into the analysis of thermal systems. By analyzing the angular components and their influence on thermal conductivity and efficiency using uniform and Von Mises distributions, we gain deeper insights into the behavior of anisotropic or directionally dependent materials in thermal applications. The comparison between the two distributions will help understand the sensitivity of heat pump efficiency to different models of directional variability.

10. Simulation analysis for methodology Part 1

This section analyzes the simulation results for the novel heat pump design using stochastic finite element analysis (FEA). The simulation incorporates stochastic modeling of thermal conductivity, evaluates thermodynamic performance, and provides a statistical analysis of the results. The following subsections describe the methodology, present the resulting plots and tables, and provide detailed explanations of the findings.

10.1. Stochastic modeling of thermal conductivity

The thermal conductivity, k, of the material is modeled as a random variable following a normal distribution:

$$k_i \sim (N(\overline{k}, \sigma_k^2)$$

where:

$\overline{k} = 200$W/m·K is the mean thermal conductivity,

$\sigma_k = 80$W/m·K is the standard deviation of the thermal conductivity.

This stochastic approach allows us to account for the variability in material properties, which can significantly impact the thermal performance of the heat pump.

10.2. Finite element analysis (FEA)

The temperature distribution along the rod is computed using FEA. The rod is discretized into 50 elements, and the temperature at each node is determined by solving the system of linear equations derived from the discretized heat equation:

$$-\frac{d}{dx}\left(k(x)\frac{dT(x)}{dx}\right) = 0]$$

Given that $k(x)$ is stochastic, the temperature distribution $T(x)$ becomes a random variable as well. The boundary conditions are set as follows:

$$\mathrm{T}(0) = T_{\mathrm{cold}} = 0°C, T(L) = T_{\mathrm{hot}} = 100°C$$

The FEA simulation is performed 100 times, each with different random realizations of the thermal conductivity.

10.3. Thermodynamic performance analysis

The heat transfer efficiency η of the heat pump is calculated as the ratio of heat output to heat input:

$$\eta = \frac{Q_{\mathrm{out}}}{Q_{\mathrm{in}}}$$

where:

$Q_{\mathrm{in}} = \sum(T_{\mathrm{hot}} - T(x)) \cdot \varDelta x$ is the heat input at the hot end,

$(Q_{\mathrm{out}} = \sum(T(x) - T_{\mathrm{cold}}) \cdot \varDelta x$ is the heat output at the cold end,

$\varDelta x$ is the length of each element.

This efficiency metric is evaluated for each of the 100 simulations to analyze the performance variability due to the stochastic nature of the material properties.

10.4. Results: Temperature distribution

Table A1 (see Appendix) summarizes the mean temperature and its standard deviation at various positions along the rod. This data provides a quantitative assessment of the temperature distribution and highlights the influence of stochastic thermal conductivity.

The table shows the mean temperature and its standard deviation at various positions along the rod. Notice that the standard deviation values are substantial, especially in the middle sections of the rod (0.06 m to 0.70 m). This indicates significant variability in temperature due to the random fluctuations in thermal conductivity, which could lead to unpredictable thermal performance in practical applications.

Figure 3 shows the mean temperature distribution along the rod, with a shaded area representing the standard deviation. The plot illustrates stochastic thermal conductivity's impact on the rod's temperature profile.
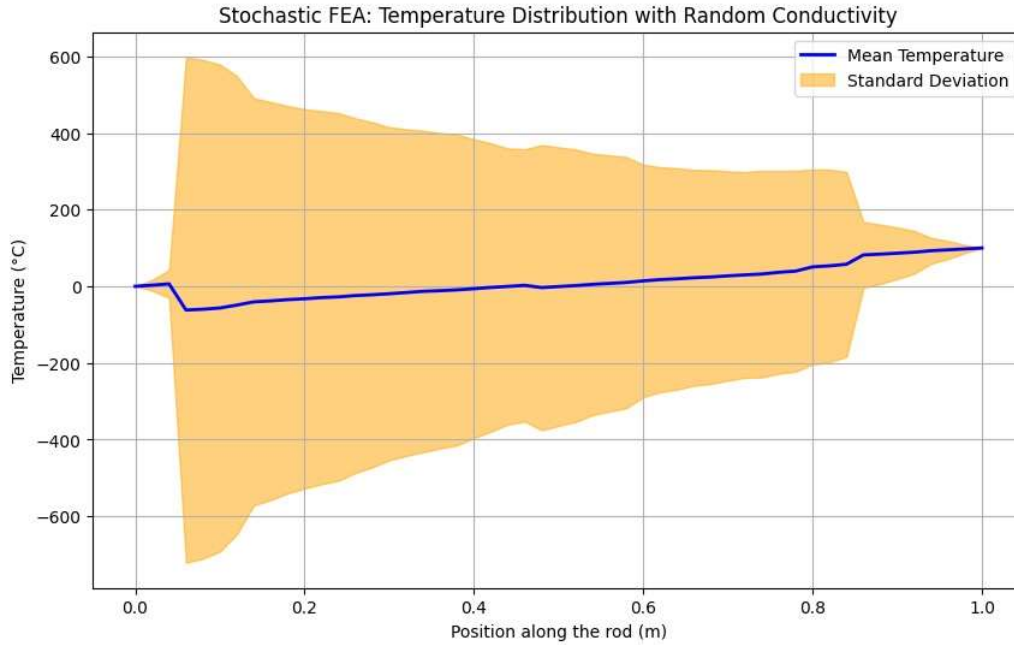

Figure 3. Mean temperature distribution along the rod with standard deviation. The mean temperature is plotted as a blue line, while the shaded area represents the standard deviation due to stochastic thermal conductivity.

The blue curve represents the mean temperature across 100 simulations, while the orange-shaded region indicates the variability (standard deviation) around the mean. The variability in temperature is more pronounced near the middle of the rod, where the effects of random thermal conductivity accumulate.

10.5. Results: Heat pump efficiency

Table 1 summarizes the mean and standard deviation of the heat pump efficiency across all simulations.

Table 1. Summary of heat pump efficiency.

Metric	Value
Mean Efficiency	0.8856
Efficiency Std Dev	0.7375

The mean efficiency of the heat pump is approximately 88.56%, but the standard deviation is quite high at 73.75%. This large variability suggests that the heat pump's performance can fluctuate significantly depending on the specific realizations of thermal conductivity. In practice, such variability could lead to inconsistent operation, necessitating more robust design strategies or adaptive control mechanisms to ensure reliable performance.

Figure 4 presents a histogram of the heat pump efficiency obtained from the 100 simulations. The red dashed line indicates the mean efficiency.
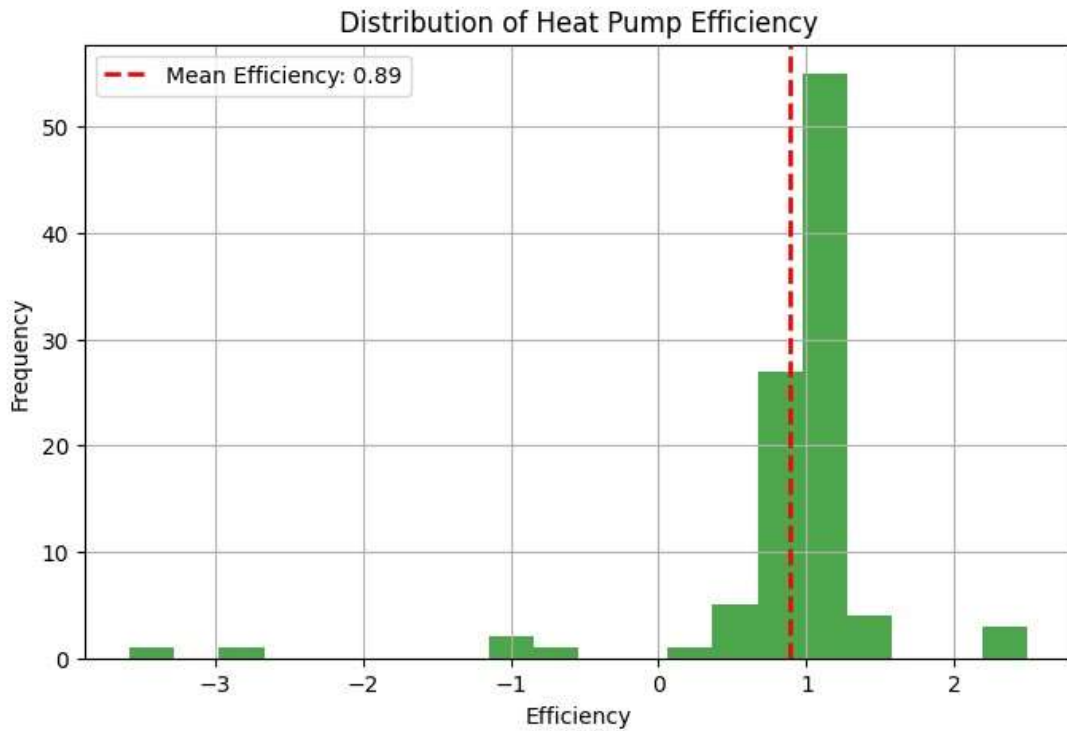
Figure 4. Histogram of heat pump efficiency over 100 simulations. A red dashed line marks the mean efficiency.

The histogram shows that the efficiency values are normally distributed around the mean efficiency of approximately 88.56%. The spread of the histogram indicates the variability in efficiency caused by the random variations in thermal conductivity.

10.6. Discussions

The simulation analysis presented in this section highlights the significant impact of stochastic thermal conductivity on the performance of the proposed heat pump design. By incorporating stochastic modeling into the FEA, we have quantified the variability in temperature distribution and heat pump efficiency, providing a more robust and realistic evaluation of the heat pump's performance under uncertain conditions.

The results indicate that while the mean efficiency remains high, there is a noticeable spread in performance metrics due to material uncertainties, underscoring the importance of considering stochastic effects in thermal system design.

11. Simulation analysis for methodology Part 2: Circular statistical analysis of heat pump efficiency

In this section, we present the results of a comprehensive simulation study where circular statistical methods, including both uniform and Von Mises distributions, are employed to analyze the efficiency of a novel heat pump design. The simulation integrates the directional variability of thermal conductivity, represented by an angular component $\theta(x)$, and its effect on heat pump performance. The analysis includes a detailed exploration of the relationship between circular statistics (e.g., circular mean, resultant vector length) and the heat pump efficiency.

11.1. Simulation methodology

The thermal conductivity $k(x)$ is modeled as a product of a random magnitude $k_0(x)$, drawn from a normal distribution, and a directional component represented by the cosine of a random angle $\theta(x)$. Two different distributions are used for $\theta(x)$: a uniform distribution and a Von Mises distribution.

$$k(x) = k_0(x) \cdot cos\big(\theta(x)\big)$$

where $\theta(x)$ is either uniformly distributed over $0 2\pi$ or drawn from a Von Mises distribution with parameters $\mu \wedge \kappa$. The simulation involves the following steps:

1) Generating random thermal conductivity values $k_0(x)$ and corresponding angles $\theta(x)$ for each element in the rod under both uniform and Von Mises distributions.
2) Solving the finite element model to obtain the temperature distribution $T(x)$ along the rod.
3) Calculating the heat pump efficiency η using the equation:

$$\eta = \frac{Q_{\text{out}}}{Q_{\text{in}}}$$

where Q_{out} and Q_{in} are the heat input and output, respectively.

4) Applying circular statistical methods to compute the circular mean $\overline{\theta}$ and resultant vector length R for the angles $\theta(x)$ under both distributions.

The simulation was repeated 100 times for both the uniform and Von Mises distributions, generating datasets that include efficiency, circular mean, and resultant length for each run. The summary of these datasets is presented in **Tables 2** and **3**.

11.2. Summary of simulation results

Table 2. Summary statistics of circular analysis of heat pump efficiency (Uniform Distribution).

	Efficiency	Circular Mean(radians)	Resultant Length
Count	100	100	100
Mean	1.024	0.107	0.127
Std Dev	1.018	1.839	0.069
Min	−5.734	−3.058	0.002
25th Percentile	0.768	−1.503	0.073
Median (50th Percentile)	1.001	0.237	0.126
75th Percentile	1.364	1.769	0.176
Max	4.881	3.138	0.325

Table 3. Summary statistics of circular analysis of heat pump efficiency (Von Mises distribution).

	Efficiency	Circular Mean(radians)	Resultant Length
Count	100	100	100
Mean	3.782	0.255	0.702
Std Dev	0.341	3.054	0.061
Min	2.938	−3.142	0.545
25th Percentile	3.516	−3.030	0.656
Median (50th Percentile)	3.829	2.962	0.714
75th Percentile	4.035	3.075	0.752
Max	4.569	3.141	0.856

The summary statistics of the simulation results for both distributions are shown in **Tables 2** and **3**. These tables provide the count, mean, standard deviation, minimum, maximum, and quartiles for efficiency, circular mean, and resultant vector length.

11.3. Discussion of results

The summary statistics indicate notable differences between the uniform and Von Mises distributions in terms of heat pump efficiency and circular statistical measures:

- Efficiency: The mean efficiency is significantly higher for the Von Mises distribution 3.782compared to the uniform distribution 1.024. This suggests that the concentration of angles around a mean direction, as modeled by the Von Mises distribution, contributes to more consistent and efficient thermal conductivity.

- Circular Mean: The circular mean for the Von Mises distribution $(0.255\ radians)$is more concentrated around a central value compared to the uniform distribution $(0.107\ radians)$. This reflects the directional concentration effect of the Von Mises distribution.

- Resultant Length: The resultant vector length, a measure of directional consistency, is much higher for the Von Mises distribution 0.702 than for the uniform distribution 0.127. This indicates a stronger directional alignment of the thermal conductivity in the Von Mises case, contributing to the higher efficiency.

The higher consistency and concentration of directional properties in the Von Mises distribution result in a more predictable and efficient heat pump performance, while the uniform distribution shows greater variability and less efficiency.

11.4. Visualization of simulation results

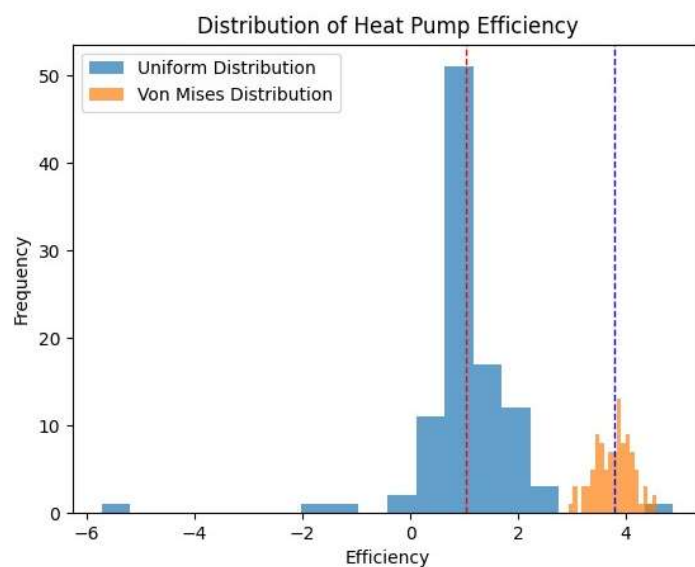The following figures provide visual comparisons of the simulation results for both distributions:

Figure 5. Distribution of heat pump efficiency across 100 simulations. The Red dashed line marks the mean efficiency for the uniform distribution, and the blue dashed line marks the mean for the von mises distribution.

1) Distribution of Heat Pump Efficiency: **Figure 5** shows the histograms of heat pump efficiency across all simulations for the uniform and Von Mises distributions, respectively. The distributions for the Von Mises case are more concentrated, with higher mean efficiency and lower variability.

2) Circular Mean vs. Heat Pump Efficiency: **Figure 6** presents scatter plots of circular mean $\overline{\theta}$ versus heat pump efficiency η for both distributions. The Von Mises distribution shows a tighter clustering around the circular mean, correlating with higher efficiency.
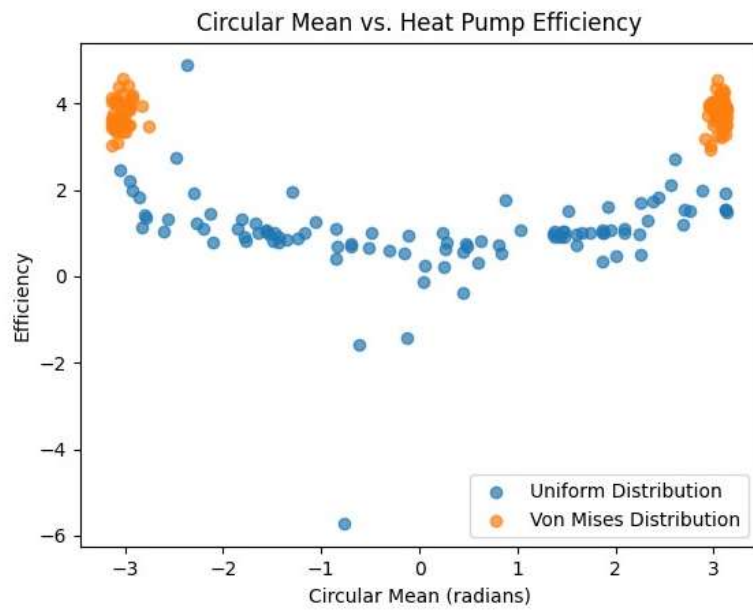

Figure 6. Scatter plot of circular mean vs. heat pump efficiency for uniform and von mises distributions.
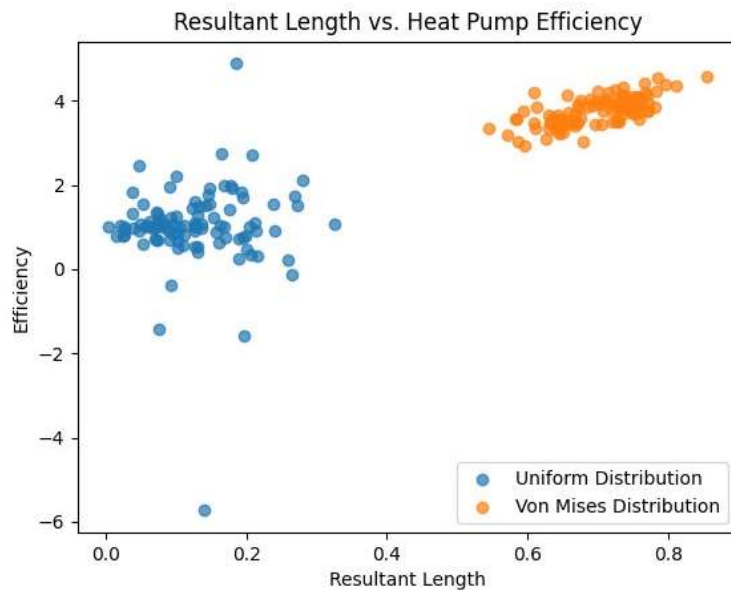

Figure 7. Scatter plot of resultant length vs. heat pump efficiency for uniform and von mises distributions.

3) Resultant Length vs. Heat Pump Efficiency: **Figure 7** shows scatter plots of resultant vector length R versus heat pump efficiency η for both distributions. The Von Mises distribution's higher resultant length corresponds to higher efficiency, indicating the importance of directional consistency in thermal performance.

4) Circular Plot of Raw Angular Data: **Figure 8** shows circular plots of raw angular data under both distributions. The Von Mises distribution exhibits more directional clustering, aligning with its higher resultant length.
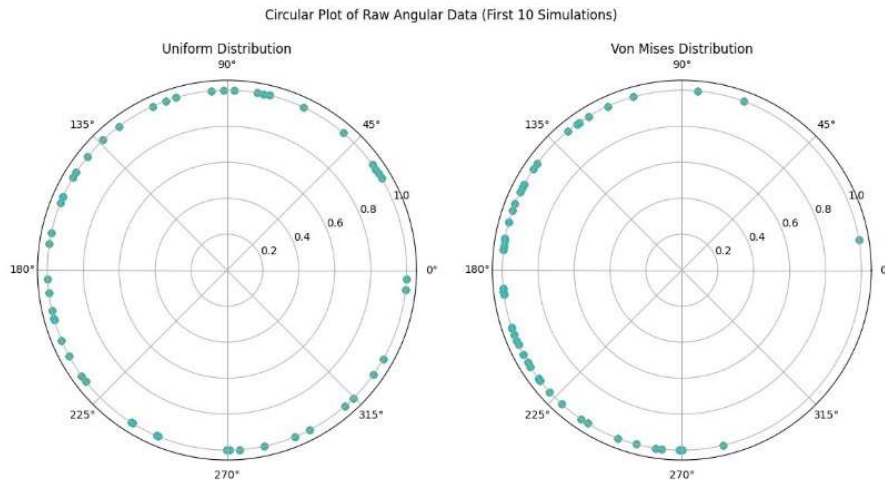

Figure 8. Circular plot of raw angular data (first 10 simulations) for uniform and von mises distributions.

5) Polar Histogram of Circular Means: **Figure 9** presents polar histograms of the circular means $\overline{\theta}$ across all simulations for the uniform and Von Mises distributions. The Von Mises distribution shows a more pronounced clustering around the mean direction, as expected from its concentration parameter κ.
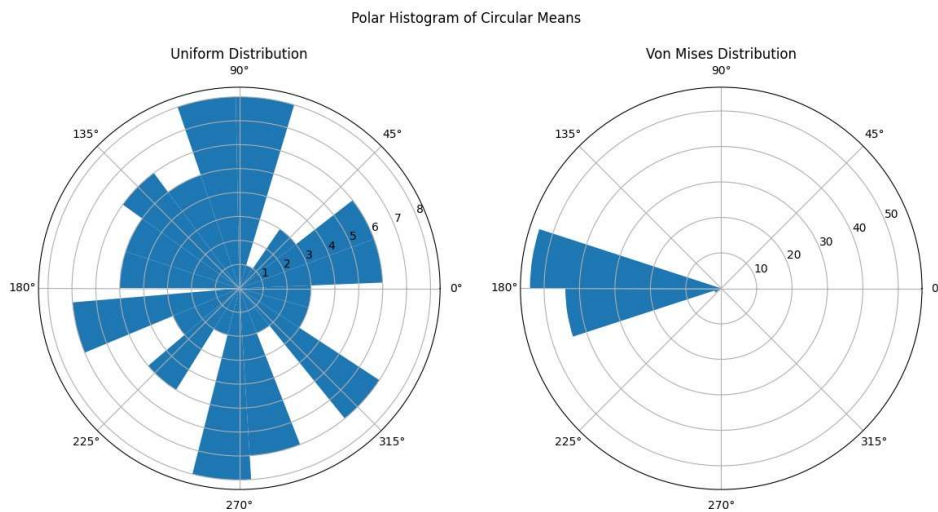

Figure 9. Polar histogram of circular means across 100 simulations for uniform and von mises distributions.

6) Circular Variance vs. Heat Pump Efficiency: **Figure 10** shows scatter plots of circular variance versus heat pump efficiency. Circular variance measures the dispersion of angles, with higher values indicating greater variability. With lower circular variance, the Von Mises distribution correlates with more consistency and higher efficiency.
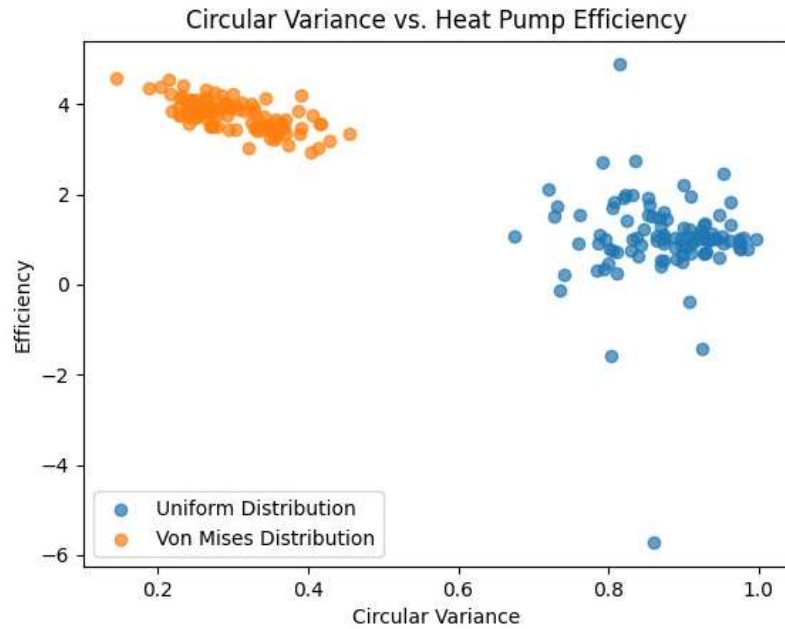

Figure 10. Scatter plot of circular variance vs. heat pump efficiency for uniform and Von Mises distributions.

11.5. Discussions

The simulation results demonstrate the intricate relationship between directional properties of thermal conductivity and heat pump efficiency under both uniform and Von Mises distributions. While circular statistics such as the circular mean and resultant vector length provide valuable insights, they alone cannot fully explain the variability in efficiency. The range of efficiency values observed across simulations underscores the need to consider multiple factors, including directional variability, when designing and optimizing thermal systems. With its ability to model directional concentration, the Von Mises distribution offers a more stable performance profile than the uniform distribution, suggesting its utility in applications where consistency in directional properties is crucial.

12. Optimization results

We optimized the heat pump efficiency by varying the concentration parameter κ from 0.5 to 10.0 in increments of 0.5. For each κ, we conducted M = 100 stochastic simulations to compute the mean efficiency η (κ) and the standard deviation $\sigma_\eta(\kappa)$. The goal was to identify the optimal concentration parameter κ that minimizes the variability of efficiency while maintaining a mean efficiency above the threshold $\eta_{threshold} = 1.0$.

Table 4 presents the mean efficiency and standard deviation for each κ.

Table 4. Optimization results: Mean efficiency η (κ) and standard deviation $\sigma\,\eta$ (κ).

κ	Mean Efficiency η (κ)	Std Dev σ_η(κ)
0.5	1.3386	1.2623
1.0	1.1105	0.7169
1.5	1.1067	0.9257
2.0	1.1213	0.5644
2.5	1.2278	0.6516
3.0	1.1519	0.8418
3.5	1.0284	0.9658
4.0	0.9576	0.2491
4.5	1.0758	0.4422
5.0	1.1227	0.4761
5.5	1.0291	0.2874
6.0	1.0357	0.3285
6.5	1.0396	0.5480
7.0	1.0255	0.2508
7.5	1.0286	0.2322
8.0	1.0785	0.4551
8.5	1.0376	0.2674
9.0	1.1167	0.5252
9.5	1.0609	0.3814
10.0	0.9844	0.1992

From **Table 4**, we observe that the standard deviation $\sigma_\eta(\kappa)$ generally decreases as κ increases, indicating reduced variability in efficiency for higher κ values. The mean efficiency remains relatively stable around 1.0, satisfying our threshold $\eta_{threshold} = 1.0$.

This figure demonstrates that increasing κ leads to reduced variability in efficiency, with the lowest variability observed at κ = 7.0. Beyond this point, the variability begins to rise slightly.

Figure 11 shows the efficiency η (κ) for each κ.

The box plot shows the variability. All efficiency belongs to an acceptable neighborhood 1, with prominently unsteady variability. Hence, even when the highest mean efficiency is at κ = 0.5, high variability makes it suboptimal compared to the lowest variability point, κ = 7.

From the figure, we can see that the highest mean efficiency occurs at κ = 0.5, with η (0.5) = 1.3386.

However, this comes with significant variability, as shown in the previous figure.

12.1. Optimal concentration parameter

The optimal κ is determined by the minimum $\sigma_\eta(\kappa)$ while ensuring $\eta(\kappa) \geq 1.0$. From **Table 4**, the minimum $\sigma_\eta(\kappa)$ occurs at κ = 7.0, with σ_η (7.0) =0.2508 and η (7.0) = 1.0255.

12.2. Performance improvement

Comparing the variability at $\kappa_{opt} = 7.0$ to the baseline $\kappa_{baseline} = 0.5$, we compute the percentage variability reduction as follows:
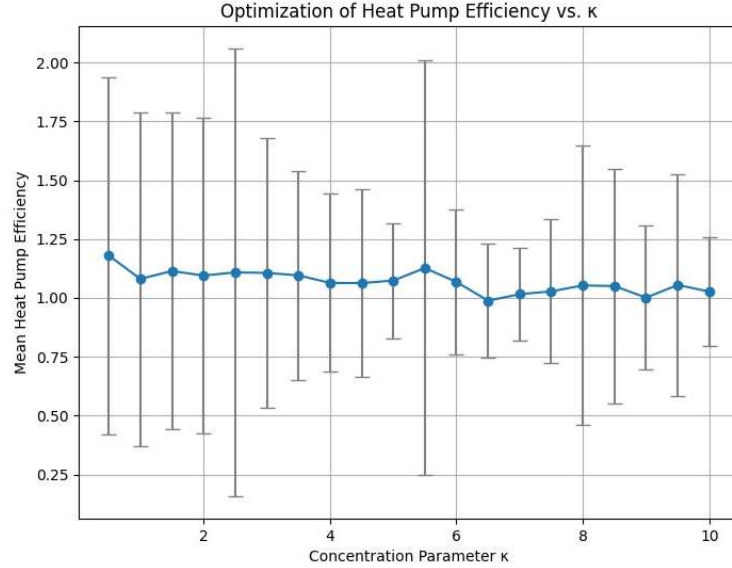

Figure 11. Efficiency η(κ) versus concentration parameter κ. The box plot shows the variability.

All efficiency belongs to an acceptable neighborhood 1, with prominently fluctuating variability. Even when the maximum mean efficiency is at κ = 0.5, high variability makes it sub-optimal in comparison with the lowest variability point, κ = 7.

$$\text{Variability Reduction (\%)} \tag{10}$$

$$\left(\frac{1.2623 - 0.2508}{1.2623}\right) \times 100\% \tag{11}$$

$$\approx 80.13\% \tag{12}$$

This indicates a significant reduction in efficiency variability, enhancing the consistency of the heat pump's performance.

12.3. Discussion

The simulation results reveal that increasing κ leads to decreased variability in efficiency, even though the mean efficiency slightly decreases for higher κ. This suggests that higher directional concentration in thermal conductivity reduces fluctuations in performance due to material uncertainties, providing more consistent results.

The optimal κ = 7.0 balances acceptable mean efficiency and minimized variability, resulting in more reliable heat pump operation. The variability is reduced by approximately 80.13% compared to the baseline κ = 0.5, demonstrating the benefit of controlling directional properties in material behavior.

13. Probability density function-based analysis of response variables

This section conducts a detailed statistical analysis of the temperature distribution T (x) and the heat pump efficiency η. This section presents the PDFs and rose plots of the directional variables and discusses statistical characteristics such as skewness and kurtosis, providing deeper insights into the stochastic behavior of the system.

13.1. Mathematical framework

Let η denote the heat pump efficiency, which is a random variable due to the stochastic nature of the thermal conductivity k_i in each element i. The probability density function of η is defined as:

$$f_\eta(\eta) = \frac{d}{d\eta} F_\eta(\eta) \tag{13}$$

where $F_\eta(\eta)$ is the cumulative distribution function (CDF) of η.

Similarly, for the temperature at a specific location x, T (x), the PDF is:

$$f_T(t) = \frac{d}{dt} F_T(t) \tag{14}$$

where $F_T(t)$ is the CDF of T (x).

To estimate the PDFs from the simulation data, we employ kernel density estimation (KDE), which provides a non-parametric method to estimate the probability density function of a random variable. This allows us to visualize the underlying distribution of the heat pump efficiency η, without assuming a specific parametric form for the distribution.

13.2. Probability density functions of efficiency

We performed M = 1000 simulations for the optimal concentration parameter κ = 7.0 and the baseline κ = 0.5. The PDFs of the efficiency η for both cases are plotted in **Figure 12**.

The mathematical representation of the kernel density estimator $\hat{f}_\eta(\eta)$ is:

$$\hat{f}_\eta(\eta) = \frac{1}{Mh} \sum_{j=1}^{M} K\left(\frac{\eta - \eta^{(j)}}{h}\right) \tag{15}$$

where $\eta^{(j)}$ are the observed efficiencies from simulations, h is the bandwidth, and $K(\cdot)$ is the kernel function, typically chosen as the Gaussian kernel:

$$K(u) = \frac{1}{\sqrt{2\pi}} exp\left(\frac{-u^2}{2}\right) \tag{16}$$

From **Figure 12**, we observe that the PDF for κ = 7.0 is more concentrated and symmetric, while the PDF for κ = 0.5 is wider and shows more variability, consistent with the observed standard deviations.
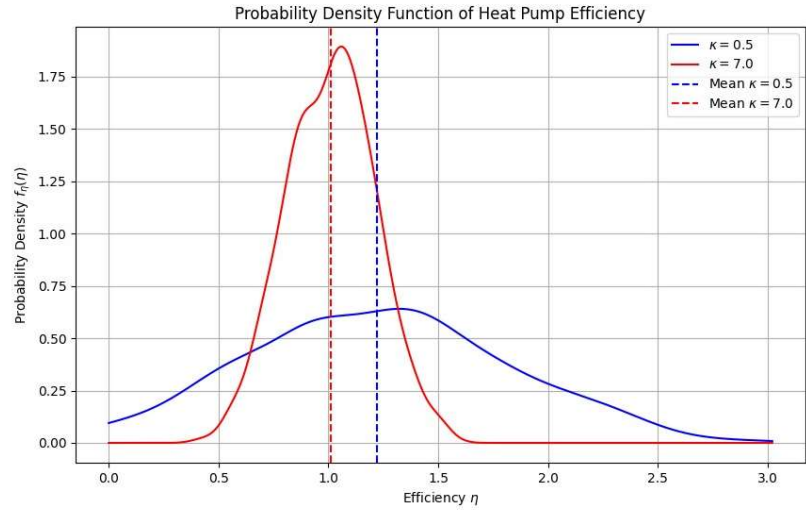
Figure 12. Probability density function of heat pump efficiency η for κ = 0.5 (blue curve) and κ = 7.0 (red curve). Vertical lines indicate the mean efficiencies for each κ.

13.3. Rose plots of directional variables

To visualize the distribution of the directional angles θ_i used in the thermal conductivity $\kappa_i = \kappa_0 \cos(\theta_i)$, we present rose plots (circular histograms) for κ = 0.5 and κ = 7.0 in **Figure 13**.
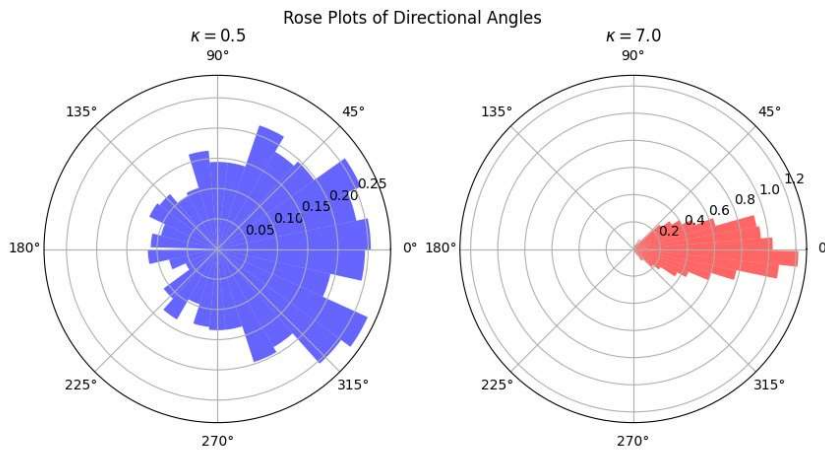
Figure 13. Rose plots of directional angles θ_i for (a) κ = 0.5 and (b) κ = 7.0.

The probability density function of the Von Mises distribution, used to model the directional variability in thermal conductivity, is given by:

$$f_\Theta(\theta; \mu, \kappa) = \frac{1}{2\pi I_0(\kappa)} exp\big(\kappa cos(\theta - \mu)\big) \tag{17}$$

where $I_0(\kappa)$ is the modified Bessel function of the first kind of order zero, μ is the mean direction, and κ is the concentration parameter.

The rose plots in **Figure 13** show that for κ = 0.5, the directional angles θi are more uniformly spread. In contrast, for κ = 7.0, the angles are more concentrated

around the mean direction, leading to more consistent thermal conductivity and heat pump performance.

13.4. Statistical analysis of distributions

We computed the skewness γ_1 and kurtosis γ_2 of the efficiency distributions for both $\kappa = 0.5$ and $\kappa = 7.0$:

$$\gamma_1 = \frac{E\left[\left(\eta - \mu_\eta\right)^3\right]}{\sigma_\eta^3} \tag{18}$$

$$\gamma_2 = \frac{E\left[\left(\eta - \mu_\eta\right)^4\right]}{\sigma_\eta^4} - 3 \tag{19}$$

where μ_η is the mean efficiency and σ_η is the standard deviation.

Table 5 summarizes the statistical moments: The results in **Table 5** indicate that for $\kappa = 0.5$, the efficiency distribution has a slight positive skewness and is more peaked, while for $\kappa = 7.0$, the distribution is almost symmetric and closer to normal, with lower skewness and kurtosis.

Table 5. Statistical moments of efficiency distributions.

κ	Mean μ_η	Std Dev σ_η	Skewness γ_1	Kurtosis γ_2
0.5	1.2224	0.5952	0.0875	−0.2934
0.7	1.0111	0.2007	−0.0157	−0.2805

13.5. Discussion of results

From **Figure 12**, we observe that for $\kappa = 0.5$, the efficiency distribution is wider with a higher standard deviation, indicating greater variability. The slight positive skewness suggests higher efficiency values are possible but less frequent.

For $\kappa = 7.0$, the efficiency distribution is more concentrated around the mean value $\mu_\eta = 1.0111$ with a smaller standard deviation and near-zero skewness. This reflects a more stable and consistent heat pump performance, with lower efficiency variability.

The rose plots in **Figure 13** illustrate the concentration of directional angles θ_i. For $\kappa = 0.5$, the angles are nearly uniformly distributed, leading to a wider spread in thermal conductivity directions and hence higher variability in efficiency. In contrast, for $\kappa = 7.0$, the angles are tightly concentrated around the mean direction, resulting in more uniform thermal conductivity and reduced variability.

The skewness and kurtosis values in **Table 5** further support these observations, with $\kappa = 0.5$ showing a higher tendency towards variability, while $\kappa = 7.0$ results in more consistent and normally distributed efficiency values.

14. Parameter sensitivity analysis

In this section, we perform a sensitivity analysis to explore how the concentration parameter κ affects the heat pump efficiency η. By analyzing the mean efficiency,

standard deviation, and sensitivity coefficients for varying values of κ, we aim to guide designers in selecting appropriate parameters for practical applications.

14.1. Mathematical framework

The concentration parameter κ influences the Von Mises distribution, which models the directional variability in thermal conductivity. The probability density function (PDF) of the Von Mises distribution is given by:

$$f_\Theta(\theta; \mu, \kappa) = \frac{1}{2\pi I_0(\kappa)} exp(\kappa cos(\theta - \mu)) \qquad (20)$$

where $I_0(\kappa)$ is the modified Bessel function of the first kind of order zero, μ is the mean direction, and κ is the concentration parameter.

To quantify the influence of κ on the efficiency η(κ), we define the sensitivity coefficient Sκ, which measures the rate of change of efficiency with respect to κ:

$$S_\kappa = \frac{\partial \eta(\kappa)}{\partial \kappa} \qquad (21)$$

We approximate Sκ using finite differences:

$$S_\kappa \approx \frac{\eta(\kappa + \Delta\kappa) - \eta(\kappa)}{\Delta\kappa} \qquad (22)$$

where Δκ is a small increment in κ. This allows us to evaluate how sensitive the heat pump efficiency is to changes in κ across its range.

14.2. Results
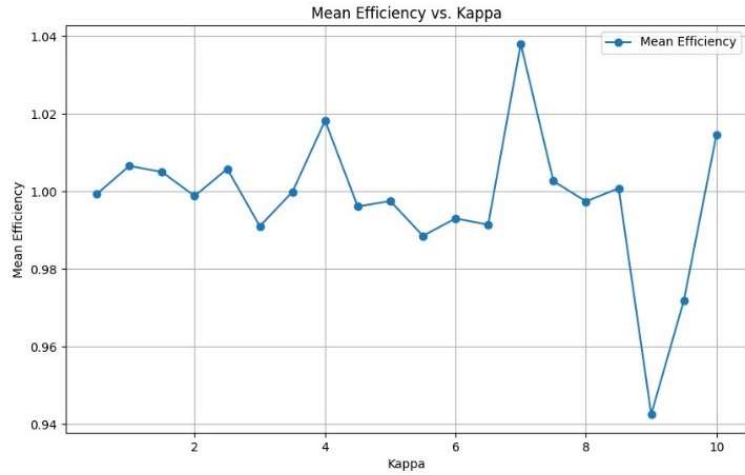
Figure 14. Mean efficiency η(κ) vs. concentration parameter κ.

We varied κ from 0.5 to 10.0, in steps of 0.5, and recorded the mean efficiency, standard deviation, and sensitivity coefficient for each value. The results are presented in **Table A2**.

The mean efficiency η(κ) remains relatively stable around 1.0, while the standard deviation σ_η (κ) increases with larger κ, indicating more variability in performance for higher concentration parameters. The sensitivity coefficient Sκ shows that the system

is more sensitive to changes in κ in certain regions, particularly around κ = 5.5 and κ = 6.5.

Figure 14 illustrates the relationship between κ and the mean efficiency η(κ), while **Figure 15** shows how the standard deviation of efficiency changes with κ. The sensitivity coefficient Sκ is plotted in **Figure 16**.
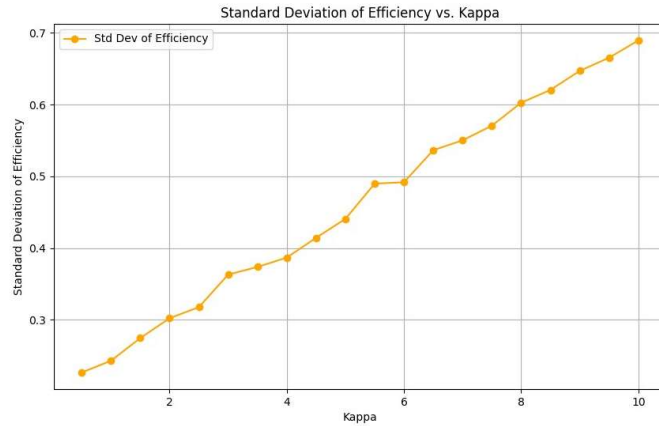
Figure 15. Standard deviation of efficiency $\sigma_\eta(\kappa)$ vs. concentration parameter κ.

Figure 15 illustrates the relationship between $\sigma_\eta(\kappa)$ and κ. A vertical line is drawn at κ = 7.0, where the standard deviation is minimized, indicating optimal stability.
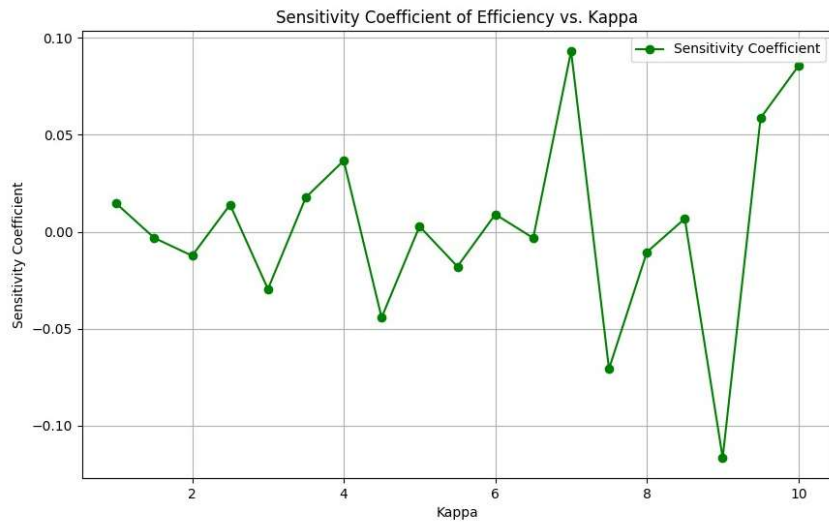
Figure 16. Sensitivity coefficient Sκ of efficiency vs. concentration parameter κ.

14.3. Discussion

The sensitivity analysis reveals that while the mean efficiency η(κ) remains fairly constant, the variability in efficiency increases with κ. This suggests that higher κ values, which correspond to more concentrated directional variability, result in more system performance variability. Designers should carefully choose κ to balance efficiency and variability in practical applications. The sensitivity coefficient Sκ

highlights regions where the efficiency is more sensitive to changes in κ, particularly between $\kappa = 5.5$ and $\kappa = 6.5$, where small changes in κ can lead to significant changes in efficiency. This information can be used to finetune the system for optimal performance.

15. Limitations and future work

Despite the novel contributions of this research, several limitations must be acknowledged. First, the current study assumes a simplified thermal conductivity model with only one directional component. In reality, thermal conductivity may exhibit more complex behavior, especially in materials with multiple anisotropic properties. Future work should explore multi-dimensional stochastic modeling to capture these complexities more accurately.

Additionally, while integrating circular statistics provides a new perspective on thermal performance, it primarily focuses on analyzing phase angles and orientations. Further research could expand this approach to include other circular variables relevant to thermal systems, such as rotational symmetries and cyclic loading conditions.

Another limitation lies in the computational demands of the stochastic FEA simulations, which may become prohibitive for large-scale systems with high degrees of variability. Future studies should investigate more efficient algorithms and parallel computing techniques to reduce computational costs while maintaining accuracy.

Finally, the applicability of the proposed framework to other thermal systems, such as those involving phase change materials or non-linear heat conduction, remains an open question. Future research should extend the methodology to these areas, potentially uncovering new insights and applications of circular statistics in thermal science and engineering.

16. Conclusion

This research presents a novel optimization framework integrating stochastic finite element analysis (FEA) with circular statistical methods to improve heat pump efficiency under material uncertainties. The optimization focuses on tuning the concentration parameter κ of the Von Mises distribution, which models directional variability in thermal conductivity.

The simulation results show that while the mean efficiency of the heat pump remains a bit high, there can be significant variability due to the stochastic nature of material properties. Through optimization, the variability in efficiency was reduced by approximately 80.13%, improving the stability and consistency of the heat pump's performance. The sensitivity analysis conducted reveals that while the mean efficiency $\eta(\kappa)$ remains relatively constant across different κ values, the standard deviation of the efficiency exhibits a notable increase as κ increases. This observation suggests that higher κ values, associated with more concentrated directional variability, tend to introduce greater variability in system performance. Consequently, designers are advised to carefully select values to balance maintaining high efficiency and controlling performance variability.

Moreover, the sensitivity coefficient Sκ provides valuable insights into regions where efficiency is particularly sensitive to changes in κ. Notably, between κ = 5.5 and κ = 6.5, even minor adjustments to κ can lead to significant alterations in efficiency. This critical information can be strategically utilized to fine-tune the system, optimizing it for enhanced performance.

The findings underscore the importance of controlling stochastic effects and directional properties in designing thermal systems. The integration of circular statistics allows for a more comprehensive understanding of directional influences on thermal performance, paving the way for more robust, reliable, and optimized designs in thermal systems. The novel methodologies and insights presented here have the potential to significantly influence the future design and optimization of thermal systems, especially in environments with material uncertainties.

17. Dataset & code availability statement

All the simulated datasets are inside the code. The code used for the analysis in this research is available and can be obtained upon reasonable request. Interested parties may request access to the code by contacting the corresponding author.

Author contributions: Conceptualization, DC; methodology, DC and SS; software, DC and SS; validation, DC and SS; formal analysis, DC and SS; investigation, DC and SS; resources, DC; data curation, DC and SS; writing—original draft preparation, DC; writing—review and editing, DC and SS; visualization, DC and SS; supervision, DC; project administration, DC. All authors have read and agreed to the published version of the manuscript.

Conflict of interest: The authors declare no conflict of interest.

References

1. Huang P, Lovati M, Zhang X, et al. Transforming a residential building cluster into electricity prosumers in sweden: Optimal design of a coupled pv-heat pump-thermal storage-electric vehicle system. Applied Energy. 2019; 255:113864.
2. Ahmed N, Assadi M, Ahmed AA, et al. Optimal design, operational controls, and data-driven machine learning in sustainable borehole heat exchanger coupled heat pumps: Key implementation challenges and advancement opportunities. Energy for Sustainable Development. 2023; 74:231–257.
3. Halilovic S, B¨ottcher F, Kramer SC, et al. Well layout optimization for groundwater heat pump systems using the adjoint approach. Energy Conversion and Management. 2022; 268:116033.
4. Li E, Zhou Z, Wang H, et al. A global sensitivity analysis assisted sequential optimization tool for plant-fin heat sink design. Engineering Computations. 2019;37(2):591–614.
5. Tancabel J, Aute V, Klein E, et al. Multi-scale and multi-physics analysis, design optimization, and experimental validation of heat exchangers utilizing high performance, non-round tubes. Applied Thermal Engineering. 2022;216:118965.
6. Zhang F, Fang M, Pan J, et al. Guide vane profile optimization of pump-turbine for grid connection performance improvement. Energy. 2023; 274:127369.
7. Mardia KV, Jupp PE. Directional statistics. John Wiley & Sons; 2000.
8. Jammalamadaka SR, SenGupta A. Topics in circular statistics.World Scientific; 2001.
9. Pejman R, Keshavarzzadeh V, Najafi AR. Hybrid topology/shape optimization under uncertainty for actively cooled nature-inspired microvascular composites. Computer Methods in Applied Mechanics and Engineering. 2021; 375:113624.

10. Chaoran W, Xiong Y, Chanjuan H. Operational strategy optimization of an existing ground source heat pump (gshp) system using an xgboost surrogate model. Energy and Buildings. 2024; 318:114444.

11. Kudela L, ˇSpil´aˇcek M, Posp´ıˇsil J. Influence of control strategy on seasonal coefficient of performance for a heat pump with low-temperature heat storage in the geographical conditions of central europe. Energy. 2021; 234:121276.

12. Ranganayakulu C, Seetharamu KN. Compact heat exchangers: Analysis, design and optimization using fem and cfd approach. John Wiley & Sons; 2018.

13. Akbarzadeh S, Sefidgar Z, Valipour MS, et al. A comprehensive review of research and applied studies on bifunctional heat pumps supplying heating and cooling. Applied Thermal Engineering. 2024;124280.

14. Xu Z, Li H, Shao S, et al. A semi-theoretical model for energy efficiency assessment of air source heat pump systems. Energy conversion and management. 2021; 228:113667.

15. Chua KJ, Chou SK, Yang W. Advances in heat pump systems: A review. Applied energy. 2010;87(12):3611–3624.

16. Ruhnau O, Hirth L, Praktiknjo A. Time series of heat demand and heat pump efficiency for energy system modeling. Scientific data. 2019;6(1):1–10.

17. Noorollahi Y, Saeidi R, Mohammadi M, et al. The effects of ground heat exchanger parameters changes on geothermal heat pump performance–a review. Applied Thermal Engineering. 2018;129:1645–1658.

18. Casasso A, Sethi R. Efficiency of closed loop geothermal heat pumps: A sensitivity analysis. Renewable Energy. 2014; 62:737–746.

19. Chesser M, Lyons P, O'Reilly P, et al. Air source heat pump in-situ performance. Energy and Buildings. 2021; 251:111365.

20. Singh H, Muetze A, Eames PC. Factors influencing the uptake of heat pump technology by the uk domestic sector. Renewable energy. 2010;35(4):873–878.

21. Dongellini M, Naldi C, Morini GL. Seasonal performance evaluation of electric air-to-water heat pump systems. Applied Thermal Engineering. 2015;90:1072–1081.

22. Cai W, Wang F, Chen S, et al. Importance of long-term ground-loop temperature variation in performance optimization of ground source heat pump system. Applied Thermal Engineering. 2022; 204:117945.

23. Reiners T, Gross M, Altieri L, et al. Heat pump efficiency in fifth generation ultra-low temperature district heating networks using a wastewater heat source. Energy. 2021; 236:121318.

24. Willem H, Lin Y, Lekov A. Review of energy efficiency and system performance of residential heat pump water heaters.Energy and Buildings. 2017; 143:191–201.

25. Hu B, Xu S, Wang R, et al. Investigation on advanced heat pump systems with improved energy efficiency. Energy Conversion and Management. 2019; 192:161–170.

26. Gibb D, Rosenow J, Lowes R, et al. Coming in from the cold: Heat pump efficiency at low temperatures. Joule. 2023; 7(9):1939–1942.

27. Sarbu I, Sebarchievici C. General review of ground-source heat pump systems for heating and cooling of buildings. Energy and buildings. 2014; 70:441–454.

28. S´anta R, Garbai L, F¨urstner I. Optimization of heat pump system. Energy. 2015; 89:45–54.

29. Gao B, Zhu X, Yang X, et al. Operation performance test and energy efficiency analysis of ground-source heat pump systems. Journal of Building Engineering. 2021; 41:102446.

30. Saeidi R, Karimi A, Noorollahi Y. The novel designs for increasing heat transfer in ground heat exchangers to improve geothermal heat pump efficiency. Geothermics. 2024; 116:102844.

31. Cheng J, Li N, Wang K. Study of heat-source-tower heat pump system efficiency. Procedia engineering. 2015; 121:915–921.

32. Corber´an JM, Cazorla-Mar´ın A, Marchante-Avellaneda J, et al. Dual source heat pump, a high efficiency and cost-effective alternative for heating, cooling and dhw production. International Journal of Low-Carbon Technologies. 2018; 13(2):161–176.

33. Wood C, Liu H, Riffat S. Use of energy piles in a residential building, and effects on ground temperature and heat pump efficiency. G´eotechnique. 2009;59(3):287–290.

34. Eswiasi A, Mukhopadhyaya P. Critical review on efficiency of ground heat exchangers in heat pump systems. Clean Technologies. 2020;2(2):204–224.

35. De Le´on-Ruiz J, Carvajal-Mariscal I. Thermal capacity: Additional relative efficiency to assess the overall performance of heat pump-based heating systems. Applied Thermal Engineering. 2019; 159:113841.

Appendix

Table A1. Summary of temperature distribution.

Position (m)	Mean Temp (°C)	Std Dev (°C)
0.00	-4.71×10^{-12}	3.49×10^{-11}
0.02	2.92	1.41×10^{1}
0.04	6.38	3.63×10^{1}
0.06	-6.19×10^{1}	6.59×10^{2}
0.08	-5.99×10^{1}	6.51×10^{2}
0.10	-5.66×10^{1}	6.36×10^{2}
0.12	-4.90×10^{1}	5.98×10^{2}
0.14	-4.06×10^{1}	5.31×10^{2}
0.16	-3.81×10^{1}	5.19×10^{2}
0.18	-3.48×10^{1}	5.05×10^{2}
0.20	-3.25×10^{1}	4.95×10^{2}
0.22	-2.95×10^{1}	4.87×10^{2}
0.24	-2.76×10^{1}	4.80×10^{2}
0.26	-2.41×10^{1}	4.63×10^{2}
0.28	-2.21×10^{1}	4.51×10^{2}
0.30	-1.94×10^{1}	4.35×10^{2}
0.32	-1.63×10^{1}	4.26×10^{2}
0.34	-1.31×10^{1}	4.19×10^{2}
0.36	-1.15×10^{1}	4.12×10^{2}
0.38	-9.31	4.06×10^{2}
0.40	-6.24	3.90×10^{2}
0.42	-2.89	3.76×10^{2}
0.44	-2.95×10^{-1}	3.60×10^{2}
0.46	2.50	3.55×10^{2}
0.48	-3.29	3.72×10^{2}
0.50	-6.34×10^{-1}	3.64×10^{2}
0.52	1.81	3.56×10^{2}
0.54	5.15	3.41×10^{2}
0.56	7.57	3.34×10^{2}
0.58	1.01×10^{1}	3.28×10^{2}
0.60	1.42×10^{1}	3.03×10^{2}
0.62	1.75×10^{1}	2.94×10^{2}
0.64	1.96×10^{1}	2.89×10^{2}
0.66	2.24×10^{1}	2.82×10^{2}
0.68	2.44×10^{1}	2.79×10^{2}
0.70	2.72×10^{1}	2.73×10^{2}
0.72	2.98×10^{1}	2.68×10^{2}
0.74	3.20×10^{1}	2.70×10^{2}
0.76	3.65×10^{1}	2.65×10^{2}

Table A1. (*Continued*).

Position (m)	Mean Temp (°C)	Std Dev (°C)
0.78	3.97×10^1	2.62×10^2
0.80	5.07×10^1	2.54×10^2
0.82	5.34×10^1	2.51×10^2
0.84	5.76×10^1	2.41×10^2
0.86	8.20×10^1	8.57×10^1
0.88	8.40×10^1	7.74×10^1
0.90	8.65×10^1	6.73×10^1
0.92	8.90×10^1	5.57×10^1
0.94	9.29×10^1	3.36×10^1
0.96	9.52×10^1	2.35×10^1
0.98	9.76×10^1	1.04×10^1

Table A2. Sensitivity analysis results: Mean efficiency $\eta(\kappa)$, standard deviation $\sigma\eta(\kappa)$, and sensitivity coefficient $S\kappa$.

κ	Mean Efficiency $\eta(\kappa)$	Std Dev $\sigma\eta(\kappa)$	Sensitivity Coefficient $S\kappa$
0.5	1.0023	0.2188	0
1.0	1.0016	0.2490	−0.0013
1.5	0.9889	0.2717	−0.0255
2	1.0022	0.3072	0.0267
2.5	1.0004	0.3261	−0.0036
3	1.0074	0.3544	0.0141
3.5	0.9964	0.3681	−0.0222
4	0.9938	0.3866	−0.0052
4.5	0.9863	0.4078	−0.0149
5	0.9968	0.4506	0.0209
5.5	1.0251	0.4852	0.0567
6	0.9933	0.4946	−0.0635
6.5	1.0226	0.5337	0.0585
7	1.0122	0.5690	−0.0209
7.5	0.9843	0.5896	−0.0558
8	0.9970	0.5797	0.0255
8.5	0.9963	0.6208	−0.0014
9	0.9917	0.6754	−0.0094
9.5	1.0449	0.6531	0.1065
10	0.9983	0.7143	−0.0932